2004

Testing density-dependent groundwater models: two-dimensional steady state unstable convection in infinite, finite and inclined porous layers

Douglas Weatherill
Flinders University, douglas.weatherill@flinders.edu.au

Craig T. Simmons
Flinders University, craig.simmons@flinders.edu.au

Clifford I. Voss
U.S. Geological Survey, cvoss@usgs.gov

Neville I. Robinson
Flinders University, neville.robinson@flinders.edu.au

Available online at www.sciencedirect.com
SCIENCE DIRECT®
Advances in Water Resources 27 (2004) 547–562
Advances in Water Resources
www.elsevier.com/locate/advwatres

Testing density-dependent groundwater models: two-dimensional steady state unstable convection in infinite, finite and inclined porous layers

Douglas Weatherill [a], Craig T. Simmons [a,*], Clifford I. Voss [b], Neville I. Robinson [a]

[a] School of Chemistry, Physics and Earth Sciences, Flinders University, GPO Box 2100, Adelaide, SA 5001, Australia
[b] US Geological Survey, 431 National Center, Reston, VA 20192, USA

Received 22 October 2002; received in revised form 28 January 2004; accepted 28 January 2004
Available online 9 April 2004

Abstract

This study proposes the use of several problems of unstable steady state convection with variable fluid density in a porous layer of infinite horizontal extent as two-dimensional (2-D) test cases for density-dependent groundwater flow and solute transport simulators. Unlike existing density-dependent model benchmarks, these problems have well-defined stability criteria that are determined analytically. These analytical stability indicators can be compared with numerical model results to test the ability of a code to accurately simulate buoyancy driven flow and diffusion. The basic analytical solution is for a horizontally infinite fluid-filled porous layer in which fluid density decreases with depth. The proposed test problems include unstable convection in an infinite horizontal box, in a finite horizontal box, and in an infinite inclined box. A dimensionless Rayleigh number incorporating properties of the fluid and the porous media determines the stability of the layer in each case. Testing the ability of numerical codes to match both the critical Rayleigh number at which convection occurs and the wavelength of convection cells is an addition to the benchmark problems currently in use. The proposed test problems are modelled in 2-D using the SUTRA [SUTRA—A model for saturated–unsaturated variable-density ground-water flow with solute or energy transport. US Geological Survey Water-Resources Investigations Report, 02-4231, 2002. 250 p] density-dependent groundwater flow and solute transport code. For the case of an infinite horizontal box, SUTRA results show a distinct change from stable to unstable behaviour around the theoretical critical Rayleigh number of $4\pi^2$ and the simulated wavelength of unstable convection agrees with that predicted by the analytical solution. The effects of finite layer aspect ratio and inclination on stability indicators are also tested and numerical results are in excellent agreement with theoretical stability criteria and with numerical results previously reported in traditional fluid mechanics literature.

Keywords: Variable-density; Convection; Benchmark; Modelling; Solute transport; Groundwater

1. Introduction

Groundwater models are commonly used to simulate flow and solute transport processes in natural groundwater systems. For a model to be useful, it must adequately represent the required physical processes and be numerically rigorous. The testing of models is carried out, in part, by comparing model performance with so-called "benchmark" problems. These are well-defined analytical, numerical, laboratory or field results with which the results of a model are compared to evaluate its performance. Clearly, the more benchmarks available for comparison, the more rigorous the testing process can be.

In certain groundwater problems, groundwater density varies as a function of the temperature and solute concentration of the fluid. These density variations often impact groundwater flow patterns. For example, when denser water lies directly over less dense water unstable density stratification may lead to free (density-driven) convection. Groundwater environments where concentration differences significantly affect flow patterns include seawater intrusion in coastal aquifers [13], saline

* Corresponding author. Fax: +61-8820-12905.
E-mail addresses: douglas.weatherill@flinders.edu.au (D. Weatherill), craig.simmons@flinders.edu.au (C.T. Simmons), cvoss@usgs.gov (C.I. Voss), neville.robinson@flinders.edu.au (N.I. Robinson).

0309-1708/$ - see front matter © 2004 Elsevier Ltd. All rights reserved.
doi:10.1016/j.advwatres.2004.01.003

Nomenclature

A	model domain aspect ratio in the x-direction, –
B	model domain aspect ratio in the y-direction, –
C	solute concentration, MM^{-1}
ΔC	concentration difference, MM^{-1}
$C_{\max}$	maximum concentration, MM^{-1}
$C_{\min}$	minimum concentration, MM^{-1}
Cr	Courant number, –
C_{v}	volumetric solute concentration, ML^{-3}
D_0	molecular diffusion coefficient of solute in water, $\mathrm{L}^2\mathrm{T}^{-1}$
g	acceleration due to gravity, LT^{-2}
H	porous layer thickness/length scale, L
$\mathrm{i} = \sqrt{-1}$	imaginary i, –
i, **j** and **k**	excitation mode of a perturbation, –
k	intrinsic permeability, L^2
L	layer horizontal length, L
L_x	layer length in x-direction, L
L_y	layer length in y-direction, L
ΔL	length/height of an element (parallel to flow), L
n	integer, –
$\mathrm{node}_{\mathrm{c}}$	central node number, –
N	maximum order of sinusoidal series, –
Nu	Nusselt number, –
p	pressure, $\mathrm{ML}^{-1}\mathrm{T}^{-2}$
PD	penetration depth, L
Pe_{g}	grid/mesh Peclet number, –
Q	solute mass flux, MT^{-1}
$R = Ra/4\pi^2$	scaled Rayleigh number, –
Ra	Rayleigh number, –
Ra_{c}	critical Rayleigh number, –
Ra_{c2}	second critical Rayleigh number, –
s, s_x and s_y	wavenumbers, –
SI	stability index (0: stable, 1: unstable), –
t	time, T
Δt	timestep increment, T
T	temperature, K
U_{c}	convective velocity, LT^{-1}
v	fluid velocity, LT^{-1}
$v_{\max}$	maximum fluid velocity, LT^{-1}
W	layer width, L
x, y and z	spatial coordinates, L
α	dispersivity, L
α_{L}	longitudinal dispersivity, L
α_{T}	transverse dispersivity, L
$\beta = \rho_0^{-1}(\mathrm{d}\rho/\mathrm{d}C)$	coefficient of density variation (with concentration), –
ϕ	angle of layer inclination above horizontal degrees
$\gamma = s/\pi$	scaled wavenumber, –
λ	wavelength of a convection cell, L
μ_0	dynamic viscosity of the fluid, $\mathrm{ML}^{-1}\mathrm{T}^{-1}$
θ	porosity, $\mathrm{L}^3\mathrm{L}^{-3}$
ρ	fluid density, ML^{-3}
ρ_0	fluid density at base reference concentration, ML^{-3}

disposal basins and salt lakes [20,21,26,27], contaminant spills, tailings ponds, and waste disposal sites [9]. A review of variable-density groundwater flow is presented by Simmons et al. [22].

To model systems with significant density variation, a density-dependent numerical simulator is required. Variable-density benchmark problems are needed to confirm the accuracy of density-dependent simulators. Currently, most simulators are tested by comparing results with three widely used benchmarks: (1) the Henry [11] saltwater intrusion problem; (2) the Elder [7] problem for complex natural convection where fluid flow is driven purely by fluid density differences; and (3) the HYDROCOIN level 1, case 5 "salt dome" problem [18]. Recently, the "salt lake" problem [21] was proposed as a new test case but further work is required to explore the validity of numerical solutions at very high density contrasts where oscillatory solutions are believed to exist. Diersch and Kolditz [6] provide an excellent discussion of the successes and limitations of currently used benchmarks and this discussion will not be repeated here. However, there are unresolved issues with the Elder [7] and Henry [11] problems that warrant a brief discussion. As pointed out by Diersch and Kolditz [6], the solutions obtained to the Elder problem by various simulation codes are dependent upon the level of grid discretization used. In particular, the number of convection cells and whether central upwelling or downwelling occurs appears to be intimately related to the discretization used. Furthermore, the Elder problem does not have exact analytical solutions nor stability criteria against which to assess model performance. Voss and Souza [25] pointed out that the Henry problem was an insufficient test for density-dependent flow simulators. Recently, Simpson and Clement [23] confirmed this using a coupled versus uncoupled strategy. They showed that the position and shape of the 50% isochlor was similar whether or not the density-coupled effects were properly accounted for. Their simulations showed that the density-dependent effects in the Henry problem are secondary to the influ-

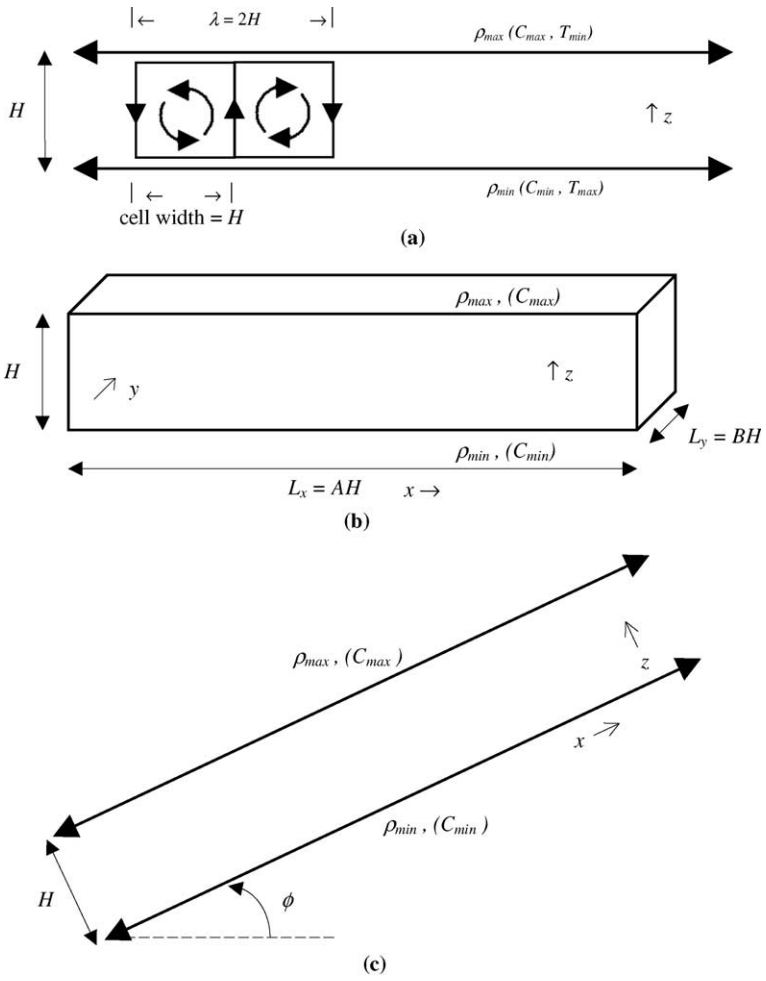

Fig. 1. (a) The Horton–Rogers–Lapwood ('infinite horizontal box') problem defined by an initial density gradient (linear for temperature, nonlinear for concentration) over layer thickness, H. Unstable cases develop convection cells of wavelength $\lambda = 2H$. (b) The 'finite horizontal box' problem with aspect ratios A and B in directions x and y. (c) The inclined layer problem ('infinite inclined box') with inclination ϕ above horizontal. C is concentration and T is temperature.

ence of the boundary forcing provided by the freshwater recharge. This implies that the Henry [11] problem is not a good test for simulators that will be applied to situations with strong density-driven flow. These points are important because the Henry and Elder problems are the most widely used test cases for benchmarking density-dependent flow models. There is clearly a need for additional benchmark cases. The aim of this paper is to describe a problem suite already studied (both analytically and numerically) for several decades in traditional fluid mechanics that demonstrates excellent potential as a 2-D benchmark test case for variable-density groundwater flow and transport simulators (with potential for extension to 3-D).

Following the work of Rayleigh [19], Horton and Rogers [12] and then Lapwood [14] independently determined the conditions necessary for free convection to occur in a porous layer of infinite horizontal extent in which fluid density decreases linearly with depth. The dimensionless Rayleigh number (Ra) determines the steady state behaviour of this variable-density system. The present study proposes some variations on the problem studied by Horton and Rogers [12] and Lapwood [14] as test cases for density-dependent numerical simulators. The test cases presented in this paper have the advantage of exact stability criteria determined analytically. In addition, the effects of aspect ratio of the porous layer and layer inclination on stability criteria may also be tested. Solutions can be separated into two distinct physical cases: (1) those that are dominated by diffusive/dispersive solute transport (stable) and (2) those where free convection is the dominant means of solute transport (unstable). Comparison of model output with the stability criteria can be used to test the performance of a variable-density flow and transport numerical simulator.

2. Problem definition

The steady state problem is defined in three parts: (i) the original infinite layer system (test case: *infinite horizontal box*) and variations to this, (ii) the finite layer (test case: *finite horizontal box*) and (iii) inclined layer (test case: *infinite inclined box*). Presented below are the problem definitions and relevant background theory.

2.1. Horizontal infinite layer ('infinite horizontal box')

The so-called Horton–Rogers–Lapwood (HRL) problem examined by Horton and Rogers [12] and independently by Lapwood [14] studies the stability of a fluid layer in porous media bounded by infinitely extending horizontal plates at the upper and lower boundaries. In the original problem definition, fluid density was assumed linearly dependent on temperature. A linear temperature gradient (highest at the bottom, lowest at the top) was defined as the difference between temperatures at the upper and lower boundaries divided by the thickness of the fluid layer ($\Delta T/H$) (Fig. 1a). For a stable solution, the pure conduction (diffusion) solution results and there is no convection. Density contours are horizontal (and infinite). When instability occurs, density contours oscillate, with clearly defined regions of upwelling and downwelling. The Rayleigh number (Ra) determines the steady state solution of the flow regime (diffusive or convective). In this study, we employ a solute analog of the thermal problem and thus define a solute Rayleigh number as the ratio of buoyancy forces (driving free convective transport of solute) to dispersive/viscous forces (that disperse solute and dissipate free convective transport), which is given by:

$$Ra = \frac{U_c H}{D_0} = \frac{\rho_0 g k \beta (C_{\max} - C_{\min}) H}{\theta \mu_0 D_0} = \frac{\text{buoyancy forces}}{\text{dispersive/viscous forces}} \tag{1}$$

where

- U_c convective velocity (LT^{-1})
- H length scale (L) taken as layer thickness in HRL problem and variations
- D_0 molecular diffusion coefficient of solute in water (L^2T^{-1})
- ρ_0 freshwater density (ML^{-3})
- g gravitational acceleration (LT^{-2})
- k intrinsic permeability (L^2)
- $\beta = \rho_0^{-1}(\partial\rho/\partial C)$ linear expansion coefficient of density/concentration (–)
- $C_{\max}$ maximum concentration (MM^{-1})
- $C_{\min}$ minimum concentration (MM^{-1})
- θ porosity (–)
- μ_0 dynamic viscosity of the fluid ($ML^{-1}T^{-1}$).

The critical Rayleigh number derived for the HRL problem (Ra_c) is $4\pi^2$ ($\sim$39.48) [17]. A perturbation to the diffusive regime will vanish in a system where $Ra < 4\pi^2$ (stable). In a system where $Ra \geqslant 4\pi^2$ a perturbation grows, generating convection cells (unstable). Square roll cells of width H form. There are two cells in one wavelength λ, which is equal to twice the layer thickness, H (Fig. 1a). For higher Rayleigh number there is a second critical value (Ra_{c2}) above which transient convection occurs, characterised by the continuous creation and disappearance of cells. Nield and Bejan [17] place Ra_{c2} in the range of 240–280 and Diersch and Kolditz [6] place it in the range 240–300. For completeness, we briefly demonstrate the occurrence of oscillatory convection. However, this study does not attempt to investigate oscillatory convection phenomena that occur at higher Rayleigh numbers. Detailed figures outlining the important flow regimes and transitional regions are presented by Caltagirone [3], Cheng [5], Gebhart et al. [10] and Nield and Bejan [17]. A comprehensive treatment of this problem is presented in Nield and Bejan [17] and the reader is referred there for further detail. Though originally derived for energy transport, the HRL problem may be converted to a solute transport analog by creating a solute sink at the lower boundary instead of a heat sink at the upper boundary (Fig. 1a).

2.2. Horizontal finite layer ('finite horizontal box')

The original problem of an infinite horizontal porous layer studied by Horton and Rogers [12] and Lapwood [14] can be modified to that of a finite porous layer by placing vertical boundaries at some horizontal spacing L apart to form a box. This modification of the boundary conditions alters the analytical criterion for system stability. The critical Rayleigh number for a three-dimensional bounded layer (Fig. 1b) with aspect ratios A and B, as presented by Caltagirone [3] is

$$Ra_c = \min_{A,B} \frac{\pi^2 \left(\frac{\mathbf{i}^2}{A^2} + \frac{\mathbf{j}^2}{B^2} + \mathbf{k}^2\right)\left(A^2\mathbf{i}^2\mathbf{k}^2 + B^2\mathbf{j}^2\mathbf{k}^2 + \left(\mathbf{i}^2 + \mathbf{j}^2\right)^2\right)}{\left(\mathbf{i}^2 + \mathbf{j}^2\right)^2} \tag{2}$$

where $A = L_x/H$, $B = L_y/H$, L_x = box length in the x-direction, L_y = box length in the y-direction and $(\mathbf{i}, \mathbf{j}, \mathbf{k})$ is the excitation mode of the perturbation.

The 2-D solution to this problem is achieved by substituting $\mathbf{j} = 0$ into the 3-D solution. The critical Rayleigh number then attains a minimum of $4\pi^2$ whenever the aspect ratio A is an integer 'n'. In all other cases $Ra_c > 4\pi^2$, and for $A < 1$, the solution approaches infinity as A tends to zero. Should layers for which $A \neq n$

become unstable, convection cells that form cannot assume their preferred square form as in the infinite layer and in the layer with an integral aspect ratio. Rather, they assume a "squashed" or "stretched" form to fill the finite domain.

2.3. Inclined infinite layer ('infinite inclined box')

A further extension to the original HRL problem is achieved by tilting, to create an inclined infinite layer (Fig. 1c). The stable solution for an inclined infinite layer differs from that for a horizontal layer in that even for low Ra, box-wide rotational flow occurs (referred to by Bories and Combarnous [1] as unicellular flow). In 3-D, the critical Rayleigh number for an inclined infinite porous layer as presented by Caltagirone [3], Cheng [5], and Gebhart et al. [10] is

$$Ra_c = \frac{4\pi^2}{\cos\phi} \tag{3}$$

where ϕ = angle of inclination above horizontal (°).

However, this solution for a 3-D system is not directly applicable to a 2-D system. Caltagirone and Bories [4] derive solutions for the transitional boundaries between the various flow regimes that occur in 3-D. A similar analysis (see Appendix A) for 2-D systems indicates that the critical Rayleigh number for convection in the x–z plane is determined by solving:

$$\det\left[[(l^2+\gamma^2)^2 - 4\gamma^2 R\cos\phi]\delta_{ll} - 16\mathrm{i}\frac{\gamma}{\pi}R\sin\phi\frac{lj}{(l^2-j^2)^2}(l^2+j^2+2\gamma^2)\delta_{l+j,\mathrm{odd}}\right] = 0 \tag{4}$$

where $l, j = 1, \ldots, N$, $\mathrm{i} = \sqrt{-1}$, δ_{lj} is the Kronecker delta function, γ is a wavenumber, det represents determinant and $R = Ra/4\pi^2$ (see Appendix A). Evaluation of the determinant in Eq. (4) produces a polynomial of order N and real coefficients from which the lowest order zero gives an approximation for Ra that improves with increasing N. Further detail is presented in Appendix A.

3. Numerical modelling

3.1. Model domain

An infinite layer cannot be modelled numerically with a finite domain method. A suitable choice of layer length is required. In accordance with the assumption of an infinite layer, it is desirable that layer length be much greater than layer depth. Furthermore, if the length of the modelled region is not to affect the resultant flow field, the choice of model domain size must be such that 'n' cells will completely fill the region (where n is an integer). Hence, the centre of downwelling/upwelling zones must occur precisely at vertical boundaries. Such a choice allows the system to develop the same number of cells per unit length that occurs in layers of infinite extent. When viewed in cross section, each convection cell appears as a flow field bounded by a square and the distance between consecutive regions (i.e. the wavelength λ) of upwelling/downwelling is equal to twice the thickness of the layer H:

$$\lambda = 2H \tag{5}$$

For these reasons, the aspect ratio, $A = L/H$, for the infinite layer cases must be an integer:

$$L = n\lambda = 2nH, \quad L \gg H \tag{6}$$

The case of the horizontal infinite layer may thus be referred to as the '*infinite horizontal box*'. For the finite layer problem, the layer length need not meet the above criterion (Eq. (6)) resulting in the variations to Ra_c described by Eq. (2). This case may be referred to as the '*finite horizontal box*'. For simplicity, the inclined infinite layer may be modelled using the criteria for the horizontally infinite problem given by Eq. (6). This case is referred to as the '*infinite inclined box*'.

3.2. Model parameters, boundary and initial conditions

Numerical simulations were performed using SUTRA (saturated–unsaturated transport), a 2-D density-dependent groundwater flow and solute transport model [24]. The model employs a 2-D finite element approximation of the governing equations in space and an implicit finite difference approximation in time. For further detail on SUTRA, the reader is referred to Voss and Provost [24] and Voss and Souza [25]. To simulate the original HRL problem, two modifications to the original problem must be implemented. Firstly, as previously discussed, because infinite layer length cannot be modelled numerically, appropriate dimensions are chosen to fulfil Eq. (6); thus the problem becomes the '*infinite horizontal box*'. Secondly, when the horizontal problems are modelled for solute rather than heat, the initial concentration solution is not linear in C. In contrast, for heat transport, the initial temperature condition is linear for a horizontal box, as mentioned earlier. The general nonlinear diffusive solutions for concentration, C, and pressure, p, for the variable-density case used as initial conditions for the solute version of the horizontal box problems are:

$$C = \frac{1}{\beta}\left[\left[1+\beta(2+\beta)\left(\frac{z}{H}\right)\right]^{\frac{1}{2}} - 1\right] \tag{7}$$

$$p = \frac{2\rho_0 gH}{3\beta(2+\beta)}\left[[1+\beta(2+\beta)]^{\frac{3}{2}} - \left[1+\beta(2+\beta)\left(\frac{z}{H}\right)\right]^{\frac{3}{2}}\right] \tag{8}$$

These solutions are independent of Ra for $Ra < Ra_c$. Further detail on Eqs. (7) and (8) is presented in Appendix B.

In practice, the most straightforward means of setting the nonlinear initial conditions in a computer simulation is not through use of the analytical solutions, described above. Rather, these solutions may be numerically generated employing $Ra < Ra_c$. Thus, a simulation with $Ra < Ra_c$ is first run to obtain the initial conditions for p and C, and the steady numerical solution (which matches Eqs. (7) and (8)) is then used as the initial condition for all cases where $Ra > Ra_c$. To obtain the steady initial nonlinear solution with $Ra < Ra_c$ from an arbitrary initial condition requires allowing the simulation to step through time until the solutions for p and C become steady. For the horizontal case, the simulated fluid velocities for the steady state initial conditions are zero. Due to the nonflowing initial condition, a perturbation (or seed) is often used to initiate convection for the horizontal box.

For the inclined layer, when $Ra > Ra_c$, the steady state fluid velocities for the initial condition describe unicellular flow and the p and C solutions are more complex, having a variation not only from top to bottom of the box, but also from end to end of the box. The steady spatial distributions of p and C are, in this case, dependent on Ra, even though $Ra < Ra_c$. Thus, there is no obvious 'quiescent' initial condition to use for the inclined case. This ambiguity in the initial condition for the infinite inclined box is irrelevant because the multicellular pattern is self-generating for this case. Thus, any unicellular initial condition may be used; however, it is preferable that the initial condition has a value of Ra only just below Ra_c for the angle of inclination being simulated in order to avoid a large change in the flow field at the initiation of the simulation for a value of $Ra > Ra_c$.

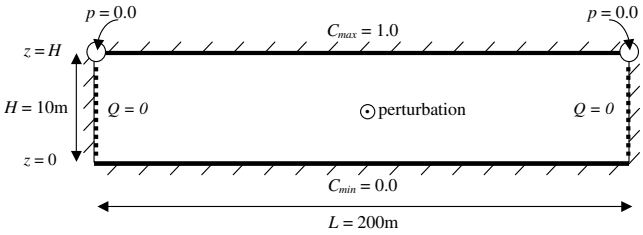

Fig. 2. Initial and boundary conditions for the 'infinite horizontal box' problem (not to scale): (1) no flow boundaries on all sides of a 10 m × 200 m box ($A = 20$), (2) specified concentration for the upper and lower boundaries, (3) no solute flux (Q) across the vertical boundaries, (4) specified pressure for the two upper corners, (5) perturbation (⊙) to the concentration field.

The boundary conditions used to simulate the problem in SUTRA are shown in Fig. 2. The horizontal box problems were modelled using a single layer depth, H (10 m) and varying layer length, L. The 'base case' parameters are listed in Table 1. For reasons irrelevant to this paper, fluid and porous medium properties were defined by close comparison with the transient Elder [7] problem for natural thermal convection using solute analog parameters employed by Voss and Souza [25]. However, matching the Rayleigh number was not a requirement and therefore the resultant Ra in the Elder problem and that employed here are different. Hence, the use of the Elder [7] parameter values was a starting point for this study from which variations in individual parameters (k, C_{max} and H) were made. The problem was modelled as a closed box, with specified pressure boundary conditions at the upper corners with any inflowing fluid having a concentration, $C = 1.0$. Compressibility of porous matrix and fluid are set to zero in all transient simulations.

Initial conditions were obtained numerically as previously described. An initial perturbation at $t = 0$ was employed to 'trigger' instability in this potentially

Table 1
'Base case' physical parameters for the HRL problem ($Ra = 26.67$)

Symbol	Quantity	Value	Units
H	Layer depth	10	m
L	Layer length	200	m
W	Layer width	1	m
C_{max}	Maximum concentration	1	–
C_{min}	Minimum concentration	0	–
θ	Porosity	0.1	–
k	Intrinsic permeability	4.845×10^{-13}	m^2
g	Gravity	9.81	$m\,s^{-2}$
D_0	Molecular diffusion coefficient	3.565×10^{-6}	$m^2\,s^{-1}$
μ_0	Dynamic viscosity of fresh fluid	1.0×10^{-3}	$kg\,m^{-1}\,s^{-1}$
$\partial\rho/\partial C$	Coefficient of density variation	200	$kg\,m^{-3}$
ρ_0	Freshwater density	1000	$kg\,m^{-3}$
α_L	Longitudinal dispersivity	0	m
α_T	Transverse dispersivity	0	m

unstable system. Without a trigger, instabilities would only form after a long time, generating from the locations of the specified pressure boundary conditions. The trigger was implemented by manually altering the concentration of the central node ($node_c$) or the node nearest the centre in the initial concentration distribution (shown as ⊙ in Fig. 2). This concentration was increased by 10% of the maximum concentration. Thus, for the base case where $C_{max} = 1.0$, the concentration of the central $node_c$ was altered from ≈0.5227 to ≈0.6227. A sensitivity analysis was carried out on the method of perturbation to determine whether this had an effect on the resultant steady state solution. Whilst altering the location of the perturbation and its magnitude relative to the initial background concentration distribution influenced the position of upwellings and downwellings in the resultant concentration field, it was not found to alter the Ra_c at which onset of instabilities occurs, nor the convective wavelength of an unstable system. However, if the initial conditions are inconsistent with a purely diffusive regime as described by Eqs. (7) and (8) (e.g. linear concentration and pressure), the potentially large initial velocities in the box may cause the steady convective wavelength to not be matched correctly.

3.3. Spatial and temporal discretization

Solute transport problems involving significant density contrasts are very sensitive to discretization [6]. The Rayleigh number defines the steady state stability of these problems. When modelling a scenario with $Ra \geqslant Ra_c$, model output should resemble free convection. Models for $Ra < Ra_c$ should produce vertically stratified concentration output for horizontal boxes, representative of solute transport caused by diffusion alone. Whilst model testing must provide confirmation that the code is correctly simulating the physical processes, it should also confirm spatial and temporal discretization is appropriately chosen. Spatial discretization is usually selected according to the grid/mesh Peclet number (Pe_g):

$$Pe_g = \frac{|v_{max}|\Delta L}{D_0 + \alpha|v_{max}|} \tag{9}$$

where v_{max} = maximum velocity parallel to ΔL (LT^{-1}), ΔL = element height or length parallel to flow (L), D_0 = molecular diffusivity in porous medium (L^2T^{-1}) and α = dispersivity (L).

Typically, diffusion is small compared with dispersion ($D_0 \ll \alpha|v_{max}|$) and Pe_g is approximated as $\Delta L/\alpha$. However, for simulation of the test problems, dispersivity is set to zero because the analytical indicator of stability (Eq. (1)) is valid only for a constant dispersion coefficient, and therefore cannot serve to benchmark cases where the dispersion is velocity dependent. The grid Peclet number for this case thus simplifies to

$$Pe_g = \frac{|v_{max}|\Delta L}{D_0} \tag{10}$$

As a guide for numerical stability, Voss [24] suggests for SUTRA, $Pe_g \leqslant 4$. This rule of thumb to obtain stability applies to cases where transport is dominated by longitudinal rather than transverse solute flux. This does not guarantee that such discretization is adequate to produce accurate results for $Pe_g \sim 4$; thus, discretization to obtain accurate and stable results may require even further refinement in the mesh. The maximum vertical fluid velocity is highly dependent on the Rayleigh number of the system. Therefore, the choice of an appropriate mesh is also dependent on the Rayleigh number. Furthermore, the choice of grid affects numerical dispersion in the model and this can be significant when a coarse grid is employed. When numerical dispersion exceeds physical dispersion, this leads to a reduction in the effective Rayleigh number being simulated in the system.

Temporal discretization is dependent on the mesh used. The Courant number (Cr) is a guide for numerical stability. Simply put, the Courant criterion requires that the advective front move only a fraction of an element per timestep. Generally, numerical stability (though, again, not necessarily accuracy) is achieved for $Cr \leqslant 1$, where

$$Cr = \frac{|v_{max}|\Delta t}{\Delta L} \tag{11}$$

where v_{max} = maximum velocity parallel to ΔL (LT^{-1}), Δt = timestep length (T) and ΔL = element length parallel to flow (L).

For the present study, grid Peclet numbers are given in Table 2 for various situations modelled using the base case parameters (Table 1), except for the varying layer depth, H. All v_{max} values were obtained post-simulation from output files. A uniform numerical grid (element length = element height = constant) was utilised for both the 'infinite horizontal box' (except simulations with $H = 12.5$ m) and for the 'infinite inclined box' problems. For 'finite horizontal box' simulations where aspect ratio was allowed to vary (up to $A = 4$), the previously used element sizes would be too large for the smaller model domain. Thus, new discretization was required for testing the effect of aspect ratio. A numerical grid using 1600 elements (80 horizontally × 20 vertically) was used in all 'finite horizontal box' simulations and was seen to produce accurate results.

For this study, all simulations utilised constant time steps and a noniterative solution method. An iterative coupling would usually be employed when modelling problems of a nonlinear nature, and would be recommended for investigation of the temporal development of the problem. In the proposed test case, however, we examine the steady state solutions only and iteration is not required. Because the model of layer depth 10 m was used for Ra up to 400, it was necessary to evaluate the

Table 2
Spatial and temporal discretization and numerical stability data for the five different layer depths (H)

	$H = 5$ m	$H = 10$ m	$H = 12.5$ m	$H = 20$ m	$H = 50$ m
Element Δz	0.5 m	1 m	1.25 m	2 m	2 m
Element Δx	0.5 m	1 m	1 m	2 m	2 m
Number of nodes	4411	2211	5226	1111	2626
Ra	13.33	26.67	33.33	53.33	133.32
Convection observed	No	No	No	Yes	Yes
Pe_g (stable $\leqslant 4$)	10^{-2}	2.8×10^{-5}	3.5×10^{-6}	0.84	1.29
Cr (stable $\leqslant 1$)	0.53	2.6×10^{-4}	2.1×10^{-5}	0.66	1.01
v_{max} (m s^{-1})	10^{-7}	10^{-10}	10^{-11}	1.5×10^{-6}	2.3×10^{-6}
Δt (s) (constant)	2,629,800	2,629,800	2,629,800	876,600	876,600

numerical stability criteria for the model under the conditions for which it is most likely to be numerically unstable. The mesh Peclet number for $Ra = 400$ was $Pe_g \approx 8.98$ for a maximum vertical velocity of 3.2×10^{-5} m s^{-1}. Although this is approximately twice the recommended maximum grid Peclet number, the simulated concentrations and velocities are reasonable. The Courant number for $Ra = 400$ is 84, far greater than the guiding value of one. All simulations were consistent in showing that with higher Ra, the system reaches equilibrium faster with respect to 0.5PD and Nu (defined in the next section). Furthermore, with higher Ra, the equilibrium values for 0.5PD and Nu are higher. Model results deviating from this trend would indicate numerical instability. A sensitivity analysis to spatial and temporal discretization clearly showed that some results were numerically erroneous where computed concentrations lay outside those specified at the upper and lower boundaries. Therefore, concentration values greater than 1.0 or less than zero are indicative of numerical error within the simulation and must be avoided. Simulations of the infinite and inclined problems utilise a grid containing 200 elements (horizontally)$\times$10 elements (vertically) (2000 elements and 2211 nodes in total). Results of a sensitivity analysis to spatial discretization are presented in Fig. 3. Grids utilising a greater number of elements in both the vertical and horizontal directions are shown in Fig. 3. Whilst small variations in Nusselt number and penetration depth are observed by increasing the grid density beyond 200×10 elements, these variations are typically less than 2% in magnitude and are therefore negligible. Thus, for the demonstration of the 2-D test cases, where there is a need to run many simulations in order to locate the transition regions between stable and unstable flow, the 200×10 element grid was used. This represented a reasonable compromise between simulation accuracy and computational effort and allowing excellent matches with both critical Rayleigh numbers and convective wavelength to be obtained.

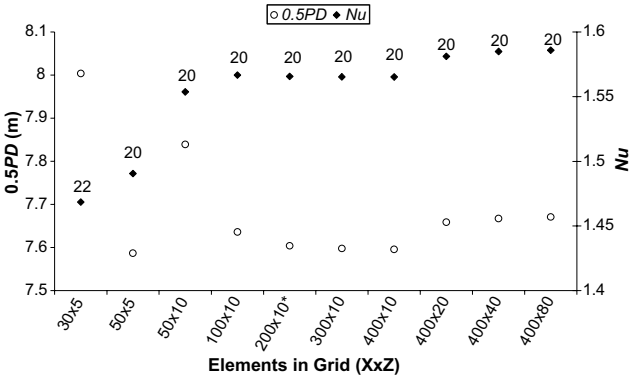

Fig. 3. Convergence analysis for spatial discretization ($Ra = 50$) showing convergence of 0.5PD, and Nu (labelled with number of convection cells) with grid refinement ($A = 20$). Solutions converge for grids with 100×10 elements (1111 nodes) or more. * denotes the grid used for the infinite and inclined parts of the test case (200×10 elements).

4. Results and discussion

4.1. A comparison of stable and unstable states

For an unstable system ($Ra \geqslant Ra_c$), instability should grow outward from the central perturbation. To indicate the stability of a system, Leijnse and Oostrom [15] used the maximum fluid velocity (v_{max}). Simmons and Narayan [20] used a stability index (SI) to classify results, where 0 is stable and 1 is unstable. The use of such an index requires judgement as to whether a system is stable or not and a time at which to assess stability states. Small instabilities may not be apparent and may be classified as stable. Rather than using a subjective stability index we utilise two quantitative indicators of stability. The first is the maximum penetration depth of the 50% concentration contour (0.5PD). This is defined to be the maximum depth at which a concentration of half of C_{max} is observed. Values were obtained via a linear interpolation based on nodal concentrations and depths. The second indicator variable is the Nusselt number at the upper boundary. The Nusselt number (Nu) is a ratio of the total mass flux through a layer (in this case the upper boundary), to diffusive flux (Eq. (12)). Theoretically, a stable system should have a Nusselt number of one, as all solute transport occurs by diffusion. Unstable systems should have $Nu > 1$, indi-

cating solute transport (convective) in addition to that caused by diffusion alone (see Nield and Bejan [17] for further detail on *Nu*).

$$Nu = \frac{Q}{D_0\theta(\Delta C_v/H)LW} \tag{12}$$

where Q = solute mass flux (MT^{-1}), D_0 = molecular diffusivity (L^2T^{-1}), θ = porosity (–), $\Delta C_v/H$ = volumetric concentration gradient across layer (ML^{-4}), L = layer length (L), and W = layer width (L).

When a system is stable, the 0.5 contour will remain at a constant depth. In an unstable system, the 0.5 contour will deviate, and will assume an oscillatory form along the length of the box.

Once a system with $Ra \geqslant 4\pi^2$ is perturbed, convection cells develop. Concentration contours deviate from the straight lines observed in a purely diffusive system. Regions where contours are closer to the upper boundary indicate upwelling. Conversely, regions where contours are closer to the lower boundary indicate downwelling (Fig. 4). As a side note, it is interesting to consider the solute fluxes within the layer. Consider the upper boundary. At no point in the model is there a greater concentration than that specified along the upper boundary. In accordance with Fick's Law, diffusion must be occurring with solute moving vertically downwards. No fluid enters the model through the upper boundary except through the specified pressure nodes (and there is essentially no flow at these points as well). Therefore, fluid circulation patterns do not correlate with solute fluxes entering/leaving the model. More solute enters the model at upwelling regions (where the diffusive gradient is higher) than that entering through downwelling regions (lower gradient). Conversely, at the lower boundary, more solute leaves the layer at regions of downwelling, and less leaves in upwelling regions. Model results (mass/solute flux across boundaries) support these observations.

Steady state concentration contours (obtained after 20 years simulation time) for a range of Rayleigh numbers (obtained by varying permeability with all other parameters fixed) are shown in Fig. 5. Clearly, $Ra = 20$ (Fig. 5a) remains stable as no convection cells are seen. $Ra = 50$ (Fig. 5b) is unstable, with concentration

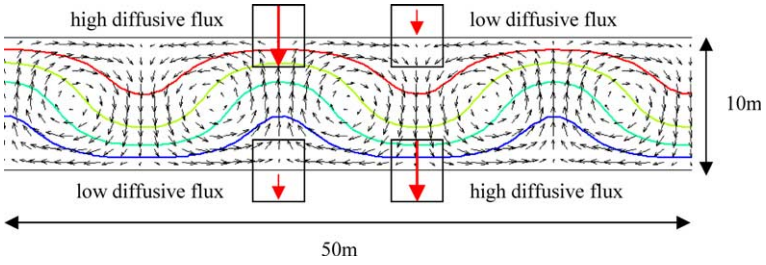

Fig. 4. The relationship between concentration contours (0.2, 0.4, 0.6 and 0.8, bottom to top) and velocity vectors for a segment of the 'infinite horizontal box' problem ($A = 20$) after 20 years ($Ra = 50$). Instability is evident in the convective circulation. Regions of upwelling and downwelling are clearly visible. Also shown are sources/sinks of solute to the convective flow pattern. Solute input at top (greatest in upwelling region); solute output at bottom (greatest in downwelling region).

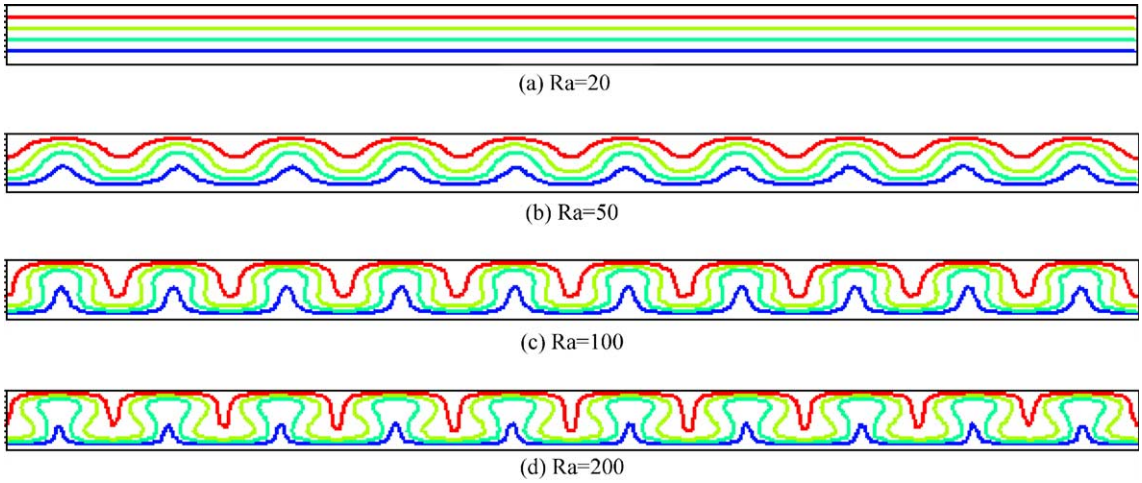

Fig. 5. 0.2, 0.4, 0.6 and 0.8 (bottom to top) concentration contours for the 'infinite horizontal box' problem ($A = 20$) after 20 years with varied intrinsic permeability corresponding to Rayleigh numbers of (a) 20 [0 cells], (b) 50 [20 cells], (c) 100 [20 cells] and (d) 200 [20 cells]. Increasing *Ra* causes concentration contours to deviate further from stable scenario positions.

contours of sinusoidal-like form. For $Ra = 100$ (Fig. 5c), the waves become flattened at the upper and lower boundaries. $Ra = 200$ (Fig. 5d) concentration contours demonstrate further flattening to the extent that some contours turn back upon themselves. Increasing Ra leads to increasingly high concentration gradients along some parts of the upper and lower boundaries. The theoretical number of cells for a layer 10 m deep and 200 m long is 20 ($\lambda = 20$ m), in exact agreement with SUTRA numerical results.

As mentioned previously, oscillatory convection can occur where Ra exceeds the range $240 < Ra < 300$. To briefly demonstrate a fluctuating oscillatory regime characterised by the continuous creation and disappearance of cells obtained for $Ra > Ra_{c2}$, a system with $Ra = 400$ was modelled at an aspect ratio of $A = 4$. SUTRA results for concentration at different times (Fig. 6) clearly depict oscillatory convection characterised by the continual breakdown and redevelopment of cells. A steady state solution is never achieved in this oscillatory mode. Consequently, the proposed test cases should be limited to cases where $Ra < 200$ to eliminate oscillatory phenomena.

4.2. Infinite horizontal box problem

The instability criterion (e.g. Ra_c) of the proposed test problems holds irrespective of the individual values of the constituent parameters in Ra. For the 'infinite horizontal box' problem, variation of three key variables were considered (intrinsic permeability, concentration difference and length scale). The Nusselt number (Nu) and the penetration depth of the 0.5 concentration contour (0.5PD) were used to analyse the growth of any subsequent instability. Fig. 7 is a stability plot that summarizes all SUTRA simulation results for the 'infinite horizontal box'. It shows the consistent transition from stable to unstable behaviour at $Ra = Ra_c = 4\pi^2$ for all SUTRA simulations, independent of which parameter is varied.

4.2.1. Intrinsic permeability

The 'infinite horizontal box' problem was modelled with a range of intrinsic permeability values corresponding to Rayleigh numbers ranging from 10 to 400. Theoretically, the value of $Ra = 4\pi^2$ should separate stable from unstable scenarios. A dramatic change is observed in 0.5PD around this critical value (Fig. 8a and b) indicating the onset of instability.

The Nusselt number changes in a similar manner to 0.5PD. Again, the value where changes to the Nusselt number occur is around $4\pi^2$ (Fig. 9a). Therefore, as Ra rises above Ra_c, convective transport is increased. It is also evident from Fig. 9a that the change in Nu with respect to changing Ra begins to taper off with increasing Ra. The greatest increase occurs for values just

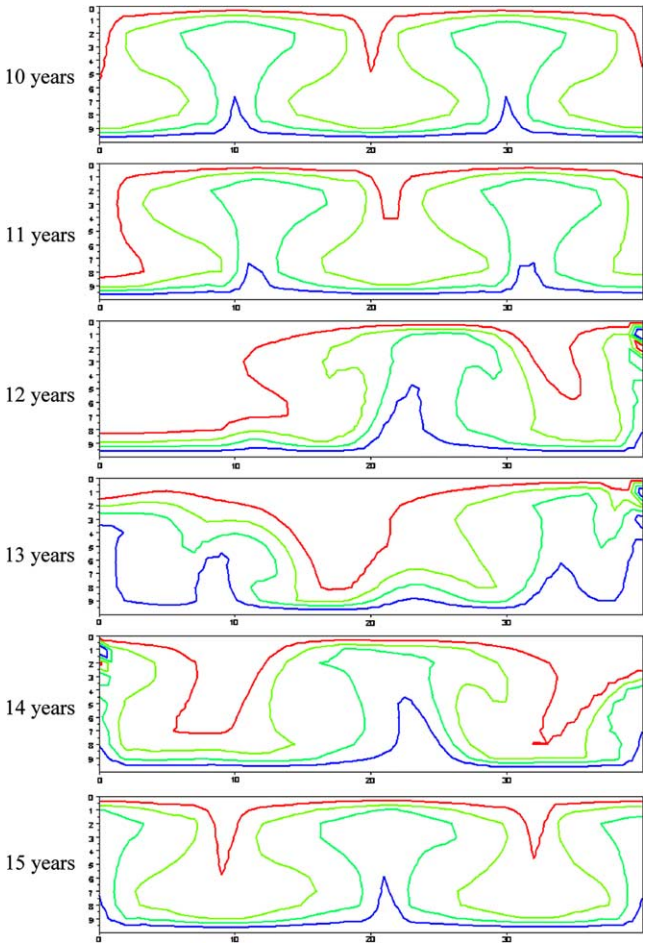

Fig. 6. Concentration contours (0.2, 0.4, 0.6 and 0.8, bottom to top) depicting oscillatory convection at 4:1 (40×10 elements) aspect ratio ($A = 4$) ($Ra = 400$). The expected 4 cells develop, but they continually break down and reform in a different arrangements. A steady state solution is not obtained.

greater than Ra_c. This is indicative of the transition between diffusive (stable) and convective (unstable) states.

4.2.2. Concentration difference

The 'infinite horizontal box' problem was modelled for a range of concentration differences. The lower boundary specified concentration was held constant at zero, while the specified concentration of the upper boundary was varied. Altering the concentration of the solute supply changes the density of the upper source boundary and hence the magnitude of the density gradient across the layer. Theory would suggest that the Rayleigh number (varied as a function of changing concentration) should again predict instability for cases where $Ra \geqslant 4\pi^2$. Using the base case parameters, Ra_c corresponds to a maximum concentration of 1.5.

In a set of simulations with varying C_{max} the 0.5 concentration contour moves up or down in the layer according to the specified C_{max} value. To keep the stable position for 0.5PD consistent between scenarios with

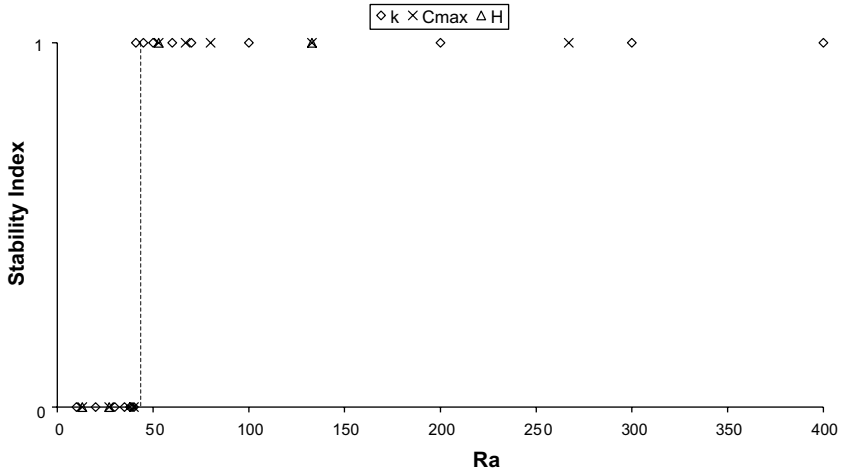

Fig. 7. Stability plot for the 'infinite horizontal box' problem ($A = 20$) for varying Ra (k, C_{max} and H). The stability index (SI) is defined to be 1 (unstable) for cases where, within 20 years, Nu increases at any time. Cases where Nu does not increase for any time within 20 years are assigned SI = 0 (stable). Note: data for the first 2 years was removed because zero fluxes were observed for very early time in some cases. Therefore, stable cases that equilibrate will show an increase in Nu for early time. Ra_c is clearly $4\pi^2$ irrespective of the variable parameter in Ra.

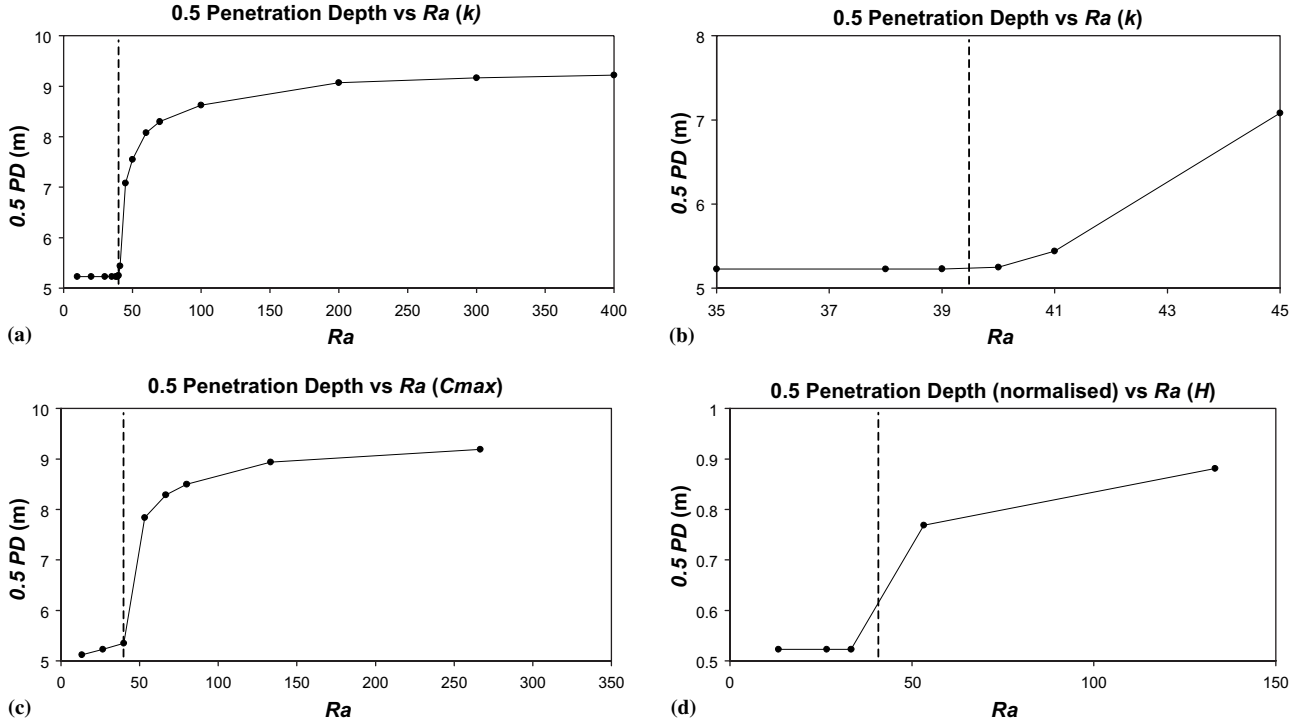

Fig. 8. 0.5PD versus Ra ($A = 20$) for varying (a) k; (b) k (details near Ra_c); (c) C_{max}; (d) H. $Ra = 4\pi^2$ is indicated by the dashed vertical line.

varying C_{max}, 0.5PD was defined in a relative sense to be the maximum depth of the concentration contour 0.5 (C_{max}), rather than the absolute 0.5 concentration contour. Results show that 0.5PD behaves identically as a function of C_{max} as it did in the varying permeability cases. The critical Rayleigh number is observed at around $4\pi^2$, above which 0.5PD varies significantly from the stable position (Fig. 8c). Higher Ra corresponds to greater equilibrium values of 0.5PD. Nusselt number data show the same trends as previously observed for permeability variation. The system again becomes unstable at a value of around $4\pi^2$ (Fig. 9b).

4.2.3. Layer depth (length scale)

The Rayleigh number incorporates a length scale (H), which is usually taken to be the depth of the layer. Numerical simulation of the 'infinite horizontal box' problem with varied layer depth was carried out, whilst

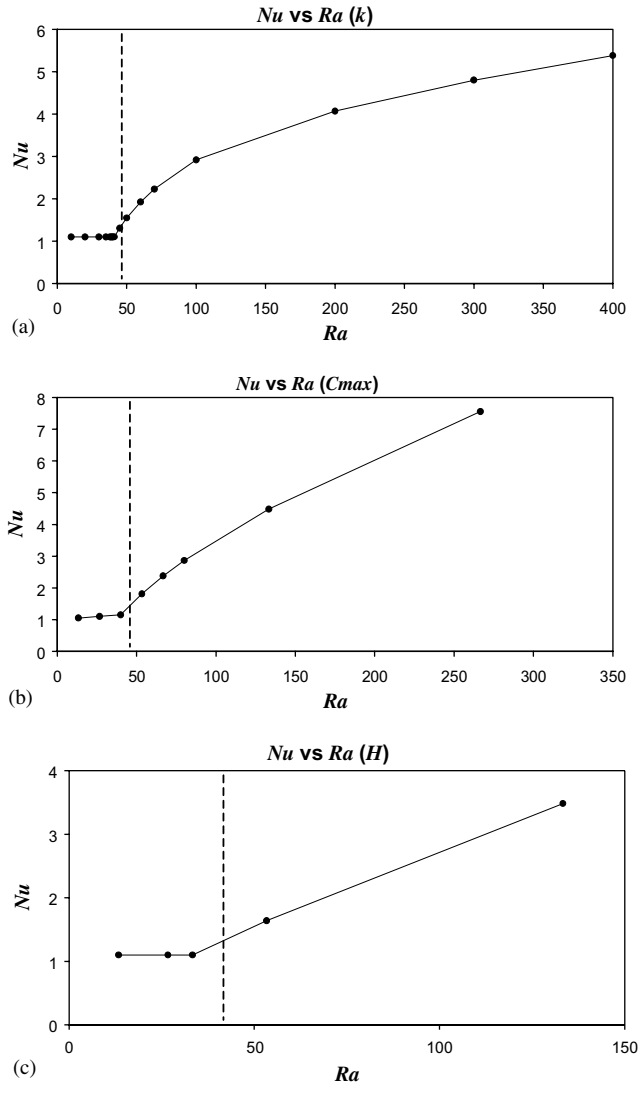

Fig. 9. *Nu* versus *Ra* ($A = 20$) for varying (a) k; (b) $C_{\max}$; (c) H. $Ra = 4\pi^2$ is indicated by the dashed line.

holding the other base case parameters constant and with numerical parameters as outlined in Table 2. Layer depths of 5, 10, and 12.5 m correspond to $Ra < 4\pi^2$, while depths of 20 and 50 m correspond to $Ra > 4\pi^2$. Results are consistent with those predicted by the critical Rayleigh number.

Penetration depths of the 0.5 concentration contour (normalised to layer depth to indicate relative divergence) are shown in Fig. 8d. For unstable cases, 0.5PD increases with increasing layer depth (even when normalised). The Nusselt number behaves similarly for layer depth as it does for permeability and concentration difference. There is no significant difference in the Nusselt number between stable cases (Fig. 9c), but changes occur for layer depths of 20 and 50 m, corresponding to Rayleigh numbers greater than $4\pi^2$.

4.3. Finite horizontal box problem

The 'finite horizontal box' problem was modelled as a laterally bounded box with varied aspect ratios from $A = 0.25$ to a maximum of $A = 4$. This was done by maintaining 'base case' conditions except for varying layer length, L. 2-D SUTRA results are consistent with the analytical stability criterion defined in Eq. (2) (Fig. 10). Ra_c increases for cases where $L \neq nH$, or more simply $A \neq n$. This is because the geometry of the box effectively forces a certain wavelength onto those regimes that become unstable. For integral aspect ratios, this wavelength is the natural wavelength of the infinite system and Ra_c is a minimum. Systems of nonintegral aspect ratio require a greater Ra_c to allow convection at the required wavelength. Model results are consistent with the analytical stability criterion that gives an increase in Ra_c towards infinity as $A \to 0$ for $A < 1$. Matching the analytical Ra_c for the region $A < 1$ is the

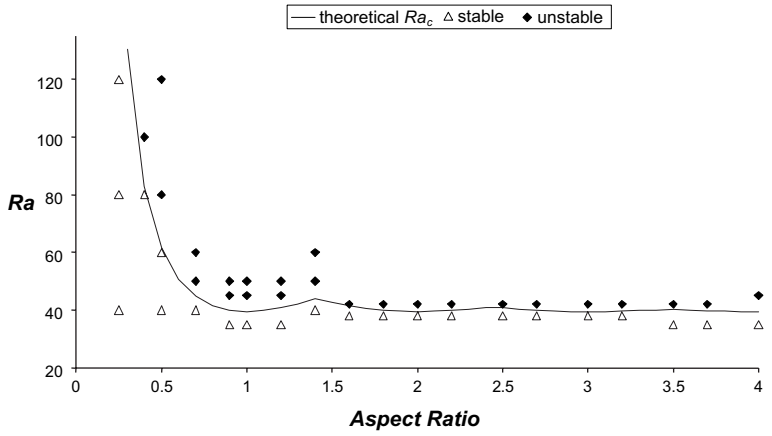

Fig. 10. Stability plot showing SUTRA results for a laterally bounded box for varying aspect ratio, A, and Ra. The analytical solution (Eq. (2)) clearly separates stable model results from those that are unstable. Little variation in Ra_c occurs for aspect ratios greater than two.

key to the test case because Ra_c is most sensitive to changes in aspect ratio in this region. Any increase in Ra_c for $A \neq n$ is small for $A > 2$ and whilst the simulations can still be tested against the Ra_c it is difficult to match the very small peaks in Ra_c. The test therefore essentially reverts to that of testing for instability when $Ra \geqslant 4\pi^2$ when $A > 1$. A further useful result follows from these observations. When modelling these horizontal box problems, it can be safely assumed that the aspect ratio of the model domain has a negligible physical effect on Ra_c if $A > 2$ and that in these cases the system behaves as if it were effectively infinite in lateral extent.

4.4. Infinite inclined box problem

The 'infinite inclined box' problem was modelled for inclinations up to $\phi = 80°$. SUTRA simulation results are in excellent agreement with the stability criteria defined in Eq. (4) and tabulated in Table 3 of Appendix A. Stable scenarios are observed as unicellular flow (one box-wide convection cell only), whilst unstable scenarios generate multiple counter-rotating cells (as in the infinite layer problem) (also see Ghebart et al. [10] for a discussion on this problem). Ra_c increases slightly up to $\phi \approx 31°$, above which Ra_c increases rapidly (Fig. 11) (see Appendix A for calculation details). Furthermore, SUTRA results are in good agreement with those obtained numerically by Caltagirone [3] for an inclined layer of $A = 4$ and $Ra = 100$. Caltagirone [3] showed a change from five to three cells at $\phi = 18°$, and a change from three cells to unicellular flow at 27.8°. These changes are reflected in abrupt changes in Nu. SUTRA results show four cells for the horizontal case (matching the theoretical wavelength exactly). A transition from three cells to unicellular flow occurs at $\phi = 31.2°$, corresponding to a rapid decrease in Nu (Fig. 12). Nu gradually increases for greater inclinations to a maximum around 70–80°

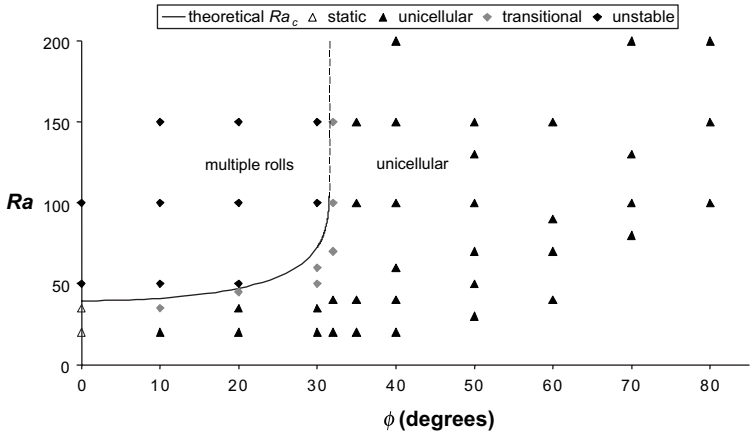

Fig. 11. Stability plot showing SUTRA results for the 'infinite inclined box' problem ($A = 20$) for varying ϕ and Ra. Results are categorised as *static*: results exhibit no fluid motion (occurs for horizontal case only); *unstable*: model results exhibit multiple counter-rotating cells; *transitional*: model results are dominated by unicellular flow with one or two extra cells just inside the lateral boundaries; *unicellular*: model results exhibit one box-wide convection cell only. Results match the theoretical Ra_c (Eq. (4)), for which the function has been extrapolated at $\phi = 31.49033°$ (dotted line).

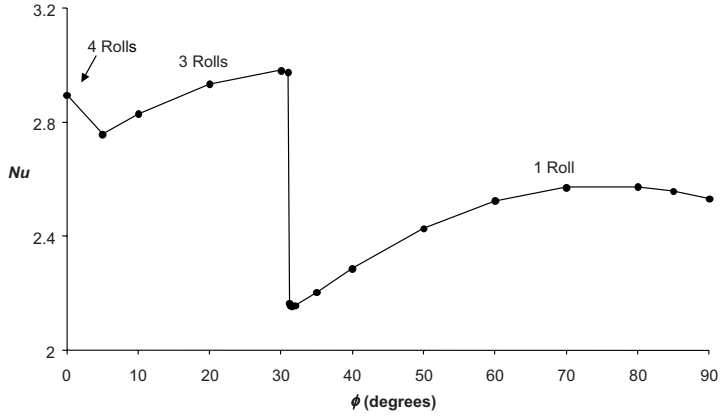

Fig. 12. Nu versus ϕ for a the 'infinite inclined box' problem modelled with SUTRA with aspect ratio, $A = 4$ and $Ra = 100$. The change from three counter-rotating cells to unicellular flow occurs at 31.2° corresponding to a large reduction in Nu.

above which there is a slight decrease. The trends observed in Fig. 12 closely match those of Caltagirone [3].

5. Summary and conclusions

This paper proposes three variations of the Horton–Rogers–Lapwood (HRL) problem as two-dimensional test cases for variable-density groundwater flow and solute transport simulators. These problems have a critical Rayleigh number Ra_c and a convective wavelength λ that can be derived analytically. Thus, these tests have the advantage of well-defined stability indicators, something not offered by any of the benchmark problems in use today (2004). The 'infinite horizontal box', 'finite horizontal box' and 'infinite inclined box' problems have been well studied analytically and numerically over the last few decades. These three problems offer an excellent opportunity for two-dimensional testing of variable-density groundwater flow and transport simulators.

As an example, the variable-density groundwater flow code, SUTRA [24] was tested on the three problems. The key results for this code are:

1. Sensitivity analyses for different constituent parameters in the Rayleigh number (intrinsic permeability, concentration difference, and layer depth) show that SUTRA matches the critical Rayleigh number Ra_c precisely in all cases and is in exact agreement with the convective wavelength λ irrespective of which parameter is varied in Ra.
2. SUTRA matches Ra_c in the most sensitive region of the analytical solution for a finite box in which $Ra_c \to$ infinity as the aspect ratio $A \to 0$ for $A < 1$.
3. SUTRA matches Ra_c as a function of layer inclination (re-derived in Appendix A following the analyses of Caltagirone and Bories [4]). Numerical results for an inclined layer demonstrate multiple counter-rotating cells for unstable scenarios and unicellular flow for stable scenarios. Also, SUTRA is in excellent agreement with the 2-D numerical results of Caltagirone [3].

Thus, three two-dimensional cases are suggested as fundamental tests of numerical codes that simulate variable-density groundwater flow. These are defined as follows.

1. Infinite horizontal box
   Geometry: Large A ($A \gg 2$, where A is an integer), horizontal.
   Objective: Match λ and Ra_c (using various combinations of system parameters to achieve the values of Ra_c as in Figs. 7–9).
2. Finite horizontal box
   Geometry: $0 < A \leqslant 2$ (A is not necessarily an integer), horizontal.
   Objective: Match Ra_c versus A, with emphasis on cases where $A < 1$ (see Fig. 10).
   Note: Numerical results suggest that for $A > 2$, Ra_c is approximately constant, closely approximating the value for the 'infinite horizontal box' case. Thus, testing should focus on the most sensitive region, where $A \leqslant 2$.
3. Infinite inclined box
   Geometry: Large A ($A \gg 2$, where A is an integer), inclined.
   Objective: Match Ra_c versus ϕ and Nu versus ϕ (see Figs. 11 and 12).

Oscillatory convection occurs at high Ra where steady state solutions are not achieved. Thus, code testing using these three problems should be limited to cases that have steady state solutions by maintaining $Ra \leqslant 200$.

Two-dimensional steady state convection in infinite boxes, in finite boxes and in inclined infinite boxes provides the basis for useful test cases and these are potential new benchmarks for variable-density groundwater flow and solute transport simulators. Well-defined solutions exist for these cases, as do other numerical results in the fluid mechanics literature. These are not currently used by the groundwater modelling community. These problems directly test the capability of a code to properly represent the steady state balance between buoyancy driven advection and diffusion. The results presented here are for 2-D simplification of 3-D systems, which have been studied in previous literature. Thus, extension of these 2-D benchmarks to 3-D situations is possible.

Acknowledgements

The authors gratefully acknowledge the assistance of Awadhesh Prasad (Murray Darling Basin Commission) for the use of his source codes to calculate the indicator variables 0.5PD and Nu. We would like to thank Christian Langevin, Barclay Shoemaker and Dorothy Tepper (U.S. Geological Survey) for their comments on an earlier version of this manuscript.

Appendix A. Critical Rayleigh number for a 2-D inclined layer

The analysis and numerical results of the 2-D inclined layer are presented briefly here because, although the analysis of Caltagirone and Bories [4] was confirmed, the definition of their tabulated numerical quantities was

not clearly defined. Caltagirone and Bories [4] describe an inclined porous layer of infinite extent in the x and y directions and unit thickness in the z-direction. The temperature of the lower boundary is held at $T = 1$ and the upper at $T = 0$. Caltagirone and Bories [4] define the following expressions for stable, unicellular flow in the system:

$$T = 1 - z; \quad v_x = Ra \sin\phi \left(\frac{1}{2} - z\right); \quad v_y = 0; \quad v_z = 0 \tag{A.1}$$

where $v_{x,y,z}$ are velocities in respective directions x, y, z.

Following standard first order perturbation procedures [17] with a use of series $\sum a_j \sin(j\pi z)$, $j = 1, \ldots, N$, exactly satisfying boundary conditions and the Galerkin method to approximately satisfy differential equations, a coefficient matrix is produced with elements, g_{lj}:

$$\begin{aligned} g_{ll} &= (l^2\pi^2 + s^2)^2 - s^2 Ra \cos\phi \\ g_{lj} &= \mathrm{i} s_x Ra \sin\phi \frac{4jl}{(l^2 - j^2)^2}\left(\frac{2s^2}{\pi^2} + l^2 + j^2\right), \\ & \quad l \pm j \text{ odd}, \quad j, l = 1, \ldots, N \end{aligned} \tag{A.2}$$

Here $s = (s_x^2 + s_y^2)^{1/2}$, s_x and s_y are the respective wavenumbers and $\mathrm{i} = \sqrt{-1}$. This is in agreement with Caltagirone and Bories [4].

The condition for instability at the critical Ra value is the determinant condition:

$$\det\lfloor g_{lj} \rfloor = 0 \tag{A.3}$$

This produces a polynomial of order N in Ra for given s, s_x, γ and ϕ. The elements g_{lj} are such that all coefficients of the polynomial are real. To obtain the leftmost curve of Caltagirone and Bories [4, Fig. 2 ($0 < \phi \leqslant 31°$)], bounding unstable convection in the x–z plane, set $s_y = 0$, i.e. $s_x = s$. To simplify the algebra, denote

$$s = \gamma\pi \quad \text{and} \quad Ra = 4\pi^2 R \tag{A.4}$$

and remove the π^4 from each row of the determinant to produce:

$$\det\left[\left[(l^2 + \gamma^2)^2 - 4\gamma^2 R \cos\phi\right]\delta_{ll} - 16\mathrm{i}\frac{\gamma}{\pi} R \sin\phi \frac{lj}{(l^2 - j^2)^2}(l^2 + j^2 + 2\gamma^2)\delta_{l+j,\mathrm{odd}}\right] = 0 \tag{A.5}$$

where δ_{lj} is the Kronecker delta function.

Determinants were calculated using a Gauss Jordan pivotal method and R was found using the Muller [16] and Frank [8] quadratic interpolation method for finding roots (not requiring derivatives). A verification was made using a symbolic algebra software package, Maple [2], for $N = 2, 3, 4, 5$, by checking the elements of the determinant and the solution for R. The variation of γ to find the minimum R was made automatic by also using a quadratic interpolation method.

Table 3
Tabulation of critical Rayleigh numbers (Ra_c) for a 2-D infinite inclined layer

ϕ	γ	$4R$	$Ra_c = 4\pi^2 R$
0	1.000000	4.000000	39.478418
5	0.998352	4.038581	39.859195
10	0.993155	4.160786	41.065316
15	0.983523	4.389775	43.325339
20	0.967418	4.782343	47.199832
25	0.939757	5.497070	54.253907
30	0.879735	7.353040	72.571595
31.4	0.829663	9.561192	94.365182

The main results are given in Table 3.

The limiting value of ϕ was found to be $\phi = 31.49033°$, and $\gamma = 0.813$. As ϕ increases, N is increased to maintain the same accuracy. For values of $\phi < 20°$, $N = 20$ will generate the accuracy tabulated. For $25° < \phi \leqslant 31.49°$, $N = 50$ was used. For $\phi > 31.49°$, $N = 90$ was used. The critical value of $\phi = 31.49033°$ was arrived at when real zeros of $\det[g_{lk}] = 0$ could no longer be found.

A comparison with the results of Caltagirone and Bories [4, Table 1] indicate that the values of their s_L, the same as γ, are in good agreement, except for a slight difference at $\phi = 20°$, where $s_L = 0.965$ whereas $\gamma = 0.967$ (also obtained at their $N = 5$ and $N = 8$). In fact γ is not very sensitive to changes in N. When $4R$ is multiplied by $\cos\phi$, there is agreement to 3 or 4 decimal places with their tabulated values of their quantity Ra_L^*. Unfortunately, Ra_L^* is not clearly defined by Caltagirone and Bories [4]. There is a slight difference in values of critical ϕ. Caltagirone and Bories [4] quote critical $\phi = 31°48' = 31.8°$ in comparison with our 31.49033°.

Appendix B. Nonlinear initial conditions

The initial concentration conditions for the HRL problem (and for the horizontal problems discussed in this paper) should give no fluid flow and only steady state diffusion of solute from top to bottom of the system. This condition is derived from the equation (the diffusive portion of the variable-density solute mass balance governing equation in terms of solute mass fraction, C (see [24]):

$$\frac{\mathrm{d}}{\mathrm{d}z}\left(\rho D_0 \frac{\mathrm{d}C}{\mathrm{d}z}\right) = 0 \tag{B.1}$$

where

$$\rho = \rho_0 + \left(\frac{\mathrm{d}\rho}{\mathrm{d}C}\right)C = \rho_0(1 + \beta C) \tag{B.2}$$

(assuming that base density, ρ_0 occurs at concentration, $C = 0$).

In contrast with the linear initial temperature condition used by HRL solutions for energy transport, the initial concentration solution is not linear in C. Solving Eq. (B.1) gives:

$$\frac{1}{2}\beta C^2 + C = \left(1 + \frac{1}{2}\beta\right)\frac{z}{H} \tag{B.3}$$

This has the linear solution, $C = z/H$, for $\beta = 0$, the constant density case.

The general concentration solution for the variable-density case, $\beta \neq 0$ is

$$C = \frac{1}{\beta}\left[\left[1 + \beta(2+\beta)\left(\frac{z}{H}\right)\right]^{\frac{1}{2}} - 1\right] \tag{B.4}$$

This also implies a nonlinear initial condition for pressure, p, which may be determined from the equation:

$$\frac{\mathrm{d}p}{\mathrm{d}z} = -\rho g \tag{B.5}$$

using the density calculated from the nonlinear initial condition for C, Eq. (B.4), by integrating:

$$\int_0^p \mathrm{d}p = -\int_H^z \rho g \,\mathrm{d}z \tag{B.6}$$

The general pressure solution for the variable-density case, $\beta \neq 0$ is

$$p = \frac{2\rho_0 g H}{3\beta(2+\beta)}\left[[1 + \beta(2+\beta)]^{\frac{3}{2}} - \left[1 + \beta(2+\beta)\left(\frac{z}{H}\right)\right]^{\frac{3}{2}}\right] \tag{B.7}$$

References

[1] Bories SA, Combarnous M. Natural convection in a sloping porous layer. J Fluid Mech 1973;57:63–79.

[2] Char BW, Geddes KO, Gonnet GH, Leong BL, Monagan MB, Watt SM. Maple V language reference manual. New York: Springer-Verlag; 1991.

[3] Caltagirone JP. Convection in a porous medium. In: Zierep J, Oertel H, editors. Convective transport and instability phenomena. Karlsruhe: G. Braun; 1982. p. 199–232.

[4] Caltagirone JP, Bories S. Solutions and stability criteria of natural convective flow in an inclined porous layer. J Fluid Mech 1985;155:267–87.

[5] Cheng P. Adv Heat Transfer 1978;14:1–105.

[6] Diersch HJG, Kolditz O. High-density flow and transport in porous media: approaches and challenges. Adv Water Resour 2002;25(8–12):899–944.

[7] Elder JW. Transient convection in a porous medium. J Fluid Mech 1967;27(3):609–23.

[8] Frank WL. Finding zeros of arbitrary functions. J Assoc Comput Mach 1958;5:154–60.

[9] Frind EO. Simulation of long term density-dependent transport in groundwater. Adv Water Resour 1982;5:73–97.

[10] Gebhart B, Jaluria Y, Mahajan RL, Sammakia B. Buoyancy-induced flows and transport. New York: Hemisphere Publishing Corporation; 1988.

[11] Henry HR. Effects of dispersion on salt encroachment in coastal aquifers. USGS Water Supply Paper 1613-C, Sea Water in Coastal Aquifers, 1964. p. C70–84.

[12] Horton CW, Rogers Jr FT. Convection currents in a porous medium. J Appl Phys 1945;16:367–70.

[13] Huyakorn PS, Andersen PF, Mercer JW, White HO. Saltwater intrusion in aquifers: development and testing of a three-dimensional finite element model. Water Resour Res 1987;23(2):293–312.

[14] Lapwood ER. Convection of a fluid in a porous medium. Proc Cambridge Philos Soc 1948;44:508–21.

[15] Leijnse A, Oostrom M. The onset of instabilities in the numerical simulation of density-driven flow in porous media. Comput Methods Water Resour 1994;X:489–96.

[16] Muller DE. A method for solving algebraic equations using an automated computer. Math Tables Aids Comput 1956;10:208–15.

[17] Nield DA, Bejan A. Convection in porous media. 2nd ed. New York: Springer-Verlag; 1999.

[18] Organisation for Economic Co-operation and Development. The International HYDROCOIN Project-Level 1: code verification. Report, Nucl. Energy Agency, Paris, 1988.

[19] Rayleigh Lord, Strutt JW. On convection currents in a horizontal layer of fluid when the higher temperature is on the under side. Philos Mag 1916;6(32):529–46.

[20] Simmons CT, Narayan KA. Mixed convection processes below a saline disposal. J Hydrol 1997;194:263–85.

[21] Simmons CT, Narayan KA, Wooding RA. On a test case for density-dependent groundwater flow and solute transport models: the salt lake problem. Water Resour Res 1999;35(12):3607–20.

[22] Simmons CT, Fenstemaker TR, Sharp JM. Variable-density groundwater flow and solute transport in heterogeneous porous media: approaches, resolutions and future challenges. J Contam Hydrol 2001;52:245–75.

[23] Simpson MJ, Clement TP. Theoretical analysis of the worthiness of the Henry and Elder problems as benchmarks of density-dependent groundwater flow models. Adv Water Resour 2003;26:17–31.

[24] Voss CI, Provost AM. SUTRA—A model for saturated–unsaturated variable-density ground-water flow with solute or energy transport. US Geological Survey Water-Resources Investigations Report, 02-4231, 2002. 250 p. Available from: http://water.usgs.gov/nrp/gwsoftware/sutra.html.

[25] Voss CI, Souza WR. Variable density flow and solute transport simulation of regional aquifers containing a narrow freshwater–saltwater transition zone. Water Resour Res 1987;23(10):1851–66.

[26] Wooding RA, Tyler SW, White I. Convection in groundwater below an evaporating salt lake: onset of instability. Water Resour Res 1997;33(6):1199–217.

[27] Wooding RA, Tyler SW, White I, Anderson PA. Convection in groundwater below an evaporating salt lake: evolution of fingers or plumes. Water Resour Res 1997;33(6):1219–28.